http://www.zju.edu.cn/jzus; E-mail: jzus@zju.edu.cn
ISSN 1009-3095 *Journal of Zhejiang University SCIENCE* V.4, No.6, P.672-682, Nov.-Dec., 2003

Analysis of tensioned membrane structures considering cable sliding*

SONG Chang-yong(宋昌永)†

(*Department of Civil Engineering, Zhejiang University, Hangzhou 310027, China*)

†E-mail: cysong@civil.zju.edu.cn

Received Oct.24, 2002; revision accepted Jan.22, 2003

Abstract: In routine design of tensioned membrane structures, the membrane is generally modeled using space membrane elements and the cables by space cable elements, with no sliding allowed between the membrane and the cables. On the other hand, large deflections are expected and sliding between the membrane and the cables is inevitable. In the present paper, the general finite element code ABAQUS was employed to investigate the influence of cable sliding on membrane surface on the structural behavior. Three analysis models were devised to fulfill this purpose: (1) The membrane element shares nodes with the cable element; (2) The cable can slide on the membrane surface freely (without friction) and (3) The cable can slide on the membrane surface, but with friction between the cable and the membrane. The sliding problem is modeled using a surface-based contact algorithm. The results from three analysis models are compared, showing that cable sliding has only little influence on the structure shape and on the stress distributions in the membrane. The main influence of cable sliding may be its effect on the dynamic behavior of tensioned membrane structures.

Key words: Membrane structures, Shape finding, Cutting pattern, Cables, Contact simulation
Document code: A **CLC number:** TU353

INTRODUCTION

Tensioned membrane structures are most suitable for use as roof structure for a variety of building types, as they provide a light, elegant, and efficient structure spanning over a large clear space (Otto, 1973). Examples include gymnasiums, exhibition centers, concert pavilions, airport terminals, etc. Tensioned membrane structures are constructed from coated fabric, rigid beams/frames, and flexible cables. According to the ways prestress is applied to the structure, tensioned membrane structures fall into two categories: pneumatic membrane structures and suspended membrane structures. When cables (boundary cables, stabilizing cables) are used to strengthen the membrane, either to stabilize the structure, or to serve as free edges in the membrane structure, the cable-membrane interaction should be included in the analysis.

The design of tensioned membrane structures consists of three stages: shape finding analysis, cutting pattern analysis, and the analysis of their structural behavior under normal climatic loads (e.g. snow load, wind load). The purpose of the shape finding analysis is to find the structure form that can satisfy the pre-defined stress system, to seek a prestress system that satisfies the configuration required by architecture. The prestress system and the structure form are inextricably linked. Any adjustments made to either one will inevitably affect the other. Many technical procedures and algorithms have been developed to find the structure form and to determine the prestress system. They can be roughly sorted into three groups: force density methods (Schek, 1974; Meek and Xia, 1999); dynamic relaxation method (Day and Bunce, 1969; Lewis and Lewis, 1996); general non-linear finite element methods (Haug and Powell, 1971; Argyris *et al.*, 1974; Bletzinger and Ramm, 1999).

During routine design of membrane struc-

* Project (G50273) supported by the Scientific Research Foundation for the Returned Overseas Scholars, Zhejiang Province

tures, the membrane is usually discretized as membrane elements and the cable as space cable elements. They are assumed to have common nodes and the relative sliding/movement between the membrane and the cables is ignored for simplicity. On the other hand, cables are not tightly connected with the membrane to avoid possible wrinkles of the membrane. Both the cable and the membrane will undergo large deformations during the shape finding procedure and during the deformation caused by external loads. Sliding between the cable and the membrane is inevitable. The sliding problem had been noticed by researchers (Matsumura *et al.*, 1997; Bletzinger and Ramn, 1999; Ishii, 1999), but has not yet been solved completely. As reviewed by Ishii (1999), only Matsumura *et al.* (1997) tackled the sliding problem by inducing 'bending' elements into the analysis of tensioned membrane structures. However, Matsumura *et al.* (1997) focused emphasis on the validity of the proposed method. No detailed analyses were performed to investigate the influence of sliding on the membrane structure behavior.

In the present paper, the sliding problem is modeled by using surface-based contact. The contact simulation can take the effects of finite sliding and the friction between the contact surfaces into consideration. To demonstrate the influences of cable sliding, the following three numerical analysis models were devised.

1) The membrane element shares nodes with the cable element (Designated as Model 1: sharing nodes);

2) The cable can slide on the membrane surface freely (without friction) (Designated as Model 2: Cable sliding but $\mu = 0.0$);

3) The cable can slide on the membrane surface, but with friction between the cable and the membrane (Designated as Model 3: Cable sliding with $\mu \neq 0$).

Numerical analyses demonstrated that cable sliding has only little influence on the structure shape and on the stress distributions in the membrane. There is also no distinct difference among the load carrying capacity of the tensioned membrane structures predicted by the three analysis models. The main influence of cable sliding is its effect on the dynamic behavior of tensioned membrane structures.

NUMERICAL SIMULATIONS FOR THE SLIDING PROBLEM

Matsumura *et al.* (1997) considered the sliding problem by introducing 'bending' elements in his analyses. The cable elements that originally coincided with one edge of the membrane elements were allowed to move into the interior of the membrane elements with or without friction. The movement destroyed the integrity of membrane elements. The method assumed that the destroyed membrane elements could bend along the cable elements; and that influence of friction could be incorporated into the analyses by introducing frictional elements between the membrane elements and the cable elements. Ishii (1999) thought the influences of the friction could be included during the finite element analyses of membrane structures by inserting springs between the membrane elements and the cable elements; no suggestions were given for the value of spring stiffness.

In the present paper, the functions available in the ABAQUS code (HKS, 2000) were utilized to investigate the sliding problem. The sliding between the membrane and the cables was modeled by using surface-based contact. Similar to ordinary analyses by the finite element method, the membranes were first discretized as space membrane elements and the cables as space cable elements. The discretized membrane elements were then defined as the slide master surface, and the cable elements as the slave surface. The master surface and the slave surface consisted of a contact pair. Mechanical surface interaction, including friction and sliding, were then introduced into the contact simulations.

The slave surface could contact with or separate (open) from the master surface during the contact simulation. When the surfaces were in contact they usually transmitted shear and normal forces across the interface. The relationship of these two force components was expressed through friction between the contacting surfaces. The friction model can be the classical isotropic Coulomb friction model; or the model established through specifying the static and/or dynamic coefficients of friction by the analyst. When the friction coefficients are zero, there is

no stress transition between the membrane elements and the cable elements. Thus the forces in the cables are constant along their length.

There are three approaches to account for the relative sliding of two surfaces in the ABAQUS (HKS, 2000). They are:

1) Finite sliding: allowing any arbitrary motion of the surfaces;

2) Small sliding: two bodies containing contact surfaces may undergo large motions, but the relative sliding of the one surface along the other is small;

3) Infinitesimal sliding and rotation: both the relative motion of the surfaces and the absolute motion of the contacting bodies are small.

In the present paper, a finite sliding model with a static coefficient of friction was employed during analyses of the tensioned membrane structures.

SHAPE FINDING ANALYSIS

The idea to perform shape finding analyses with the finite element code ABAQUS in this paper is similar to that provided by Argyris *et al*. (1974). First, the controlled points or edges were projected into the plane or some arbitrary specification of geometry, which usually consisted of several planes for ease of data generation. After the finite elements and prestress distributions were devised for the plane structures, the controlled points (edges) were then moved to the specified space locations step by step. The increments for each step could be determined by the code automatically, or could be specified by the analyst. Due to the forced displacements at the controlled points, large unbalanced forces were induced in the system. They were eliminated by the Newton-Raphson iteration method, which guaranteed the next step to start from an equilibrium state. A hypothetical material with a linear stress-strain constitution law up to very large strains was assumed. To make sure that final prestress distributions after shape finding procedure did not deviate much from the desired prestress distributions, for example, uniform prestress states, the modulus of the membrane material and the cables were assumed to be smaller by several orders (Argyris *et al*., 1974). Sometimes, small moduli values cause numerical problems, e.g. divergence of iterations, singularity of the structure. The alternative is to use increased values of the material modulus. This will in turn cause the stress distributions in the structure after shape finding to deviate from the required prestress states. The remedy is to repeat the shape finding analysis by specifying the desired prestress distributions again on the obtained configuration. In general, shape finding analysis is an iterative procedure. Several numerical attempts are required. The efficiency of this method depends on the extent of the compatibility of the specified prestress distributions and the assumed structure configuration.

Two reference membrane structures were employed in the present paper to demonstrate the shape finding procedure with the ABAQUS code. The first was a structure in which the membrane material was stretched on two coaxial rigid rings with radius $a = 10$ m and $b = 50$ m respectively (Fig. 1a). The distance between the two rings was $h = 22.924$ m. From the viewpoint of differential geometry, if the membrane material is assumed to be isotropic and the prestress is uniform, the formed surface will be a minimum surface (Otto, 1973). The analytical expression is

$$z = -a\left[\ln\left(\sqrt{x^2+y^2}+\sqrt{x^2+y^2-a^2}\right)-\ln a\right]+h$$

The shape finding with the ABAQUS code started from the plane state, with the inner ring being heightened gradually. Fig. 1b shows the perspective view of the final shape – minimum surface. Fig. 1c shows that the numerical results agreed well with the analytical results. As the modulus of the membrane was assumed to be very small during the shape finding analysis, the final stress distribution was exactly the same as that of the required prestress states.

The second example is the shape finding of the hyperbolic paraboloid (Fig. 2). The membrane is stretched among four continuous non-planar rigid oblique beams, with stabilization cable added between points B and D. Geometric parameters are shown in Fig. 2, while material properties and prestress systems are assumed to be:

Membrane-Tension: 4 N/mm; Thickness (t): 1 mm; $Et = 500$ N/mm; $v = 0.4$

Cable-Tension force: 10 kN; Cross-section area (A): 100 mm^2; $E = 2.0 \times 10^5$ MPa

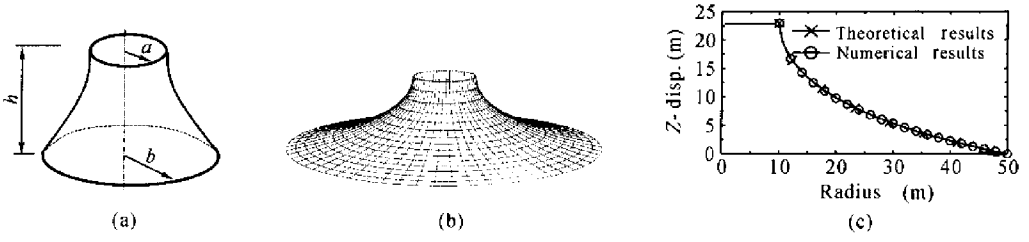

Fig.1 Minimum surface for the tensioned membrane structure
(a) schematic; (b) perspective view; (c) comparison of numerical and theoretical results

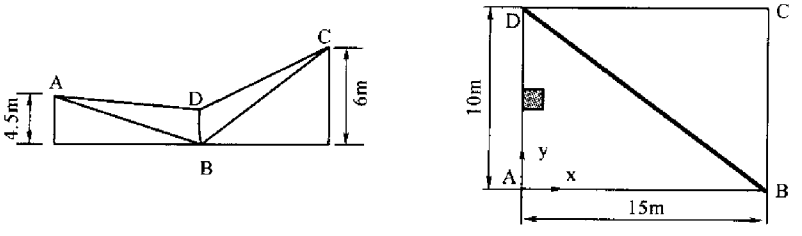

Fig.2 Schematic view of hyperbolic paraboloid

The stress-strain curves for the membrane material exhibit strong non-linearity. They possess the characteristics of visco-elastic material. Many experimental tests and numerical attempts had been carried out to describe the behavior of the membrane material (e.g. see references in Minami *et al.*, 1997; Ishii, 1999). Due to the complexity and the difficulty, and the uncertainty involved in properly describing the behavior of the membrane material, simplified constitutive laws, such as that of isotropic, orthotropic, anisotropic elastic body, have been employed according to the purposes of the calculation and the requirements of the analysis accuracy. As the objective of the present study was to investigate the influence of cable sliding on the structure behavior, the theory of an isotropic elastic body was then adopted.

The process of shape finding for the hyperbolic paraboloid was similar to that of the first example. Two analysis models were considered. One assumed that the membrane elements shared the nodes with the cable elements (Model 1). The other permitted frictionless sliding between the membrane and the cable (Model 2). Young's modulus for the membrane and the cable were assumed to be (Et) 5 N/mm and (E) 2.0×10^2 MPa respectively during the shape finding analyses. They were determined after numerical tests. For each analysis model, two rounds of shape finding analyses were performed to obtain a satisfactory geometric shape and satisfactory prestress distributions. The first round of shape finding analysis started from the plane position, while the second round of shape finding analysis was based on the geometric shapes obtained after the first round of shape finding analysis.

Fig. 3 compares the vertical coordinates of the nodes along two diagonals AC and BD after

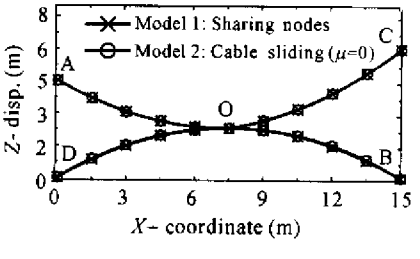

Fig.3 Effects of analysis models on the shape finding

the first round of shape finding. Fig.4 shows the perspective views of the structure with Model 1 and Model 2. Cable sliding can been seen clearly in Fig. 4b; the maximum relative slides between the cable and the membranes are 278 mm and 195 mm along and transverse to the cable respectively. On the other hand, Figs. 3 – 4 also demonstrate that sliding between the cable and the membrane had little influence on the struc-

ture configuration, though the structure underwent large deformation and large strain.

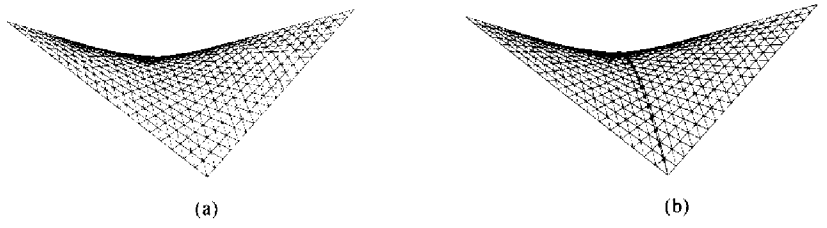

Fig.4 Perspective views of the membrane structures based on (a) Model 1: sharing nodes and (b) Model 2: cable sliding ($\mu = 0$)

Fig.5 shows the variation of the forces in the cable for two models. For Model 1, the cable forces varied with the cable length. The maximum deviation of the cable force from the initial forces was about 12%. While for Model 2, the cable force was constant along the entire length as the coefficient of friction was assumed to be zero. For the membrane, the minimum and the maximum principal stresses are 3.90 N/mm and 5.25 N/mm respectively for both models. Compared to the initial value (4 N/mm), the deviation was about 30%. The large deviation of the stress distributions is due to the large strains induced during the shape finding analyses as they started from very crude initial configurations – plane structures. The second round of shape finding analysis was performed to optimize the stress distributions. The analysis started from the configurations obtained in the first round of shape finding analysis. The initial prestress states were assumed to be 4 N/mm for the membrane and 10 kN for the cable. After the second round of shape finding, the maximum deviation of the stresses in the membrane and in the cable from the initial prestress states was only 3%. Fig.6 shows the vertical displacements occurring in the second round of shape finding analysis along the two diagonals AC and BD. The maximum vertical coordinate adjustment of the structure is 12.5 mm. Compared with the displacements which occurred in the first round of shape finding analysis, the deformations in the second round of shape finding analysis are small. They have no influence on the perspective view of the final structure configurations. To save space, only the shapes after the first round of analysis are shown in Fig.4.

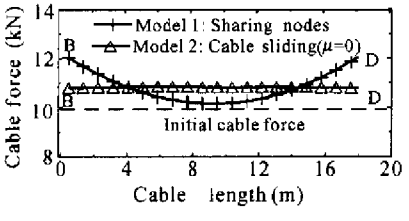

Fig.5 Variation of cable forces along the length

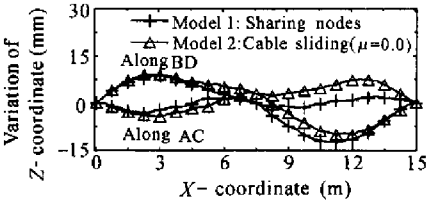

Fig.6 Variation of Z-coordinates along AC and BD after the second round of shape finding analysis

LOAD DEFLECTION ANALYSIS

The load deflection analyses that followed was based on the determined shape and the stress distributions after the second round of shape finding analysis. The three above-mentioned analysis models, together with three load cases, was addressed in detail. The three assumed load cases were uniformly distributed upward loads (LC1), uniformly distributed downward loads (LC2), and downward loads uniformly distributed on area ABD (Fig.2)(LC3). The load cases were ideal, but they have close connection with the load conditions in practical

structures, such as those of self-weight loads, snow loads and wind loads.

For Model 3, the friction coefficient should be specified prior to the analyses. It is better to determine it by experiments. Due to the lack of experimental data, it is assumed to be 0.7 as the value had been used by Matsumura *et al*. (1997).

1. Criteria of failure

During the load deflection analysis, both the membrane elements and the cable elements were assumed to be compressive stress-free. They were implemented in the ABAQUS code through modifying the linear elasticity of the material. As a first approximation, the principal stresses were obtained by assuming linear elasticity for the material. If they were found to be characterized by compression, e.g., cable sagging, membrane wrinkling, the corresponding component of the principal stresses was set to zero, and the associated stiffness matrix components were also set to zero. When enough numbers of elements connected with an element node were subjected to compressive stresses, the structure was deemed unstable; so the ultimate load carrying capacity of the tensioned membrane structures was determined through non-linear load-deflection analysis. The maximum load to which the structure was subjected before the numerical singularity was detected was taken as the ultimate load that the structure could sustain.

The definition of the cable sagging for the three models has a little difference. For Model 1, the cable sagging means that one of the cable elements is under compressive forces. While for Model 2 and Model 3, it means that the cable elements that originally was in contact with the membrane elements lost contact (or opened), and the tensile forces in the cable were zero eventually.

In Model 1, as the cable elements were assumed to share nodes with the membrane elements, cable sagging alone will not cause a numerical singularity. The ultimate load carrying capacity was determined by the performance of the membrane. On the other hand, loss of cable tension in cable-reinforced or cable-stabilized membrane structures results in relatively large deformations of the membrane and causes the membrane to wrinkle prematurely. Therefore, the cables were required to be in tension during normal service periods and cable sagging was defined as the limit state of serviceability. For Model 2 and Model 3, the cable elements and the membrane elements have independent nodes, the criteria of the failure of the membrane structures are either membrane wrinkling or cable sagging, whichever appears first.

2. Influence of cable sliding on stress distributions

Table 1 compares the load carrying capacity of the membrane structure predicted by the three analysis models. Material non-linearity was not included in the analysis.

Table 1 Influence of the analysis models on load carrying capacity (kN/m^2)

	Model 1	Model 2	Model 3
LC1	0.94 (Wrinkling)	0.94 (Wrinkling)	0.95 (Wrinkling)
LC2	0.31/0.89 (Sagging/wrinkling)	0.32 (Sagging)	0.32 (Sagging)
LC3	0.54/0.70 (Sagging/wrinkling)	0.62 (Sagging)	0.64 (Sagging)

For LC1, as the tensile forces in the cable increased with increased upward loads, cable sagging did not happen. The ultimate loads were determined by the membrane behavior, the three analysis models presented identical results. For LC2 and LC3, cable sagging happened first, the ultimate loads for Model 2 and Model 3 were the loads corresponding to the incipient appearance of cable sagging. While for Model 1, it was determined by membrane wrinkling, which occurred under much higher load level.

Table 1 shows that if membrane wrinkling appeared prior to cable sagging, the analysis models only had little influence on the ultimate load carrying capacity, or, analysis models did not have much influence on the stress states of the membrane (Figs. 7 – 8). Figs. 7 – 8 compare the stress distributions in the zone near the cable that was expected to have most significant difference. Two load levels were addressed to observe the development of the principal stresses, as well as the influences of the analysis models on the membrane behavior at different load levels. One closed to the ultimate load. The oth-

er was about half of the ultimate load. Minimum and maximum principal stresses were important for the membrane structures as they have close connection with the membrane wrinkling phenomena and the load carrying capacity corresponding to the material strength.

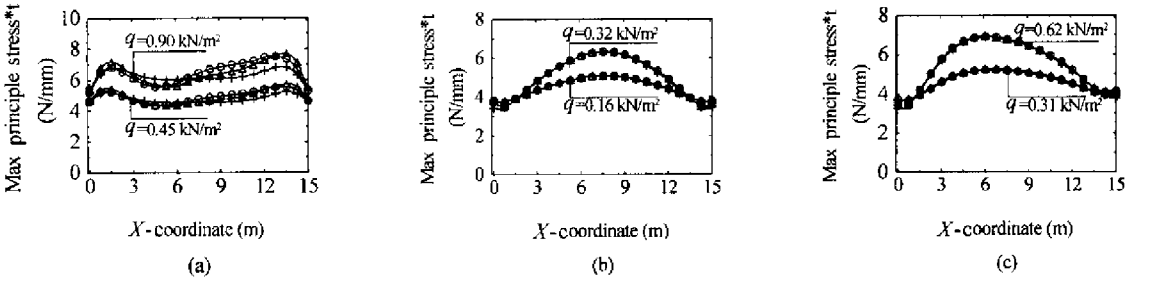

Fig.7 Maximum principle stress distributions along diagonal BD (near the cable) in the three load cases (a) LC1, (b) LC2 and (c) LC3

—+— Model 1: Sharing nodes; —△— Model 2: Cable sliding ($\mu = 0$); —○— Model 3: Cable sliding ($\mu = 0.7$)

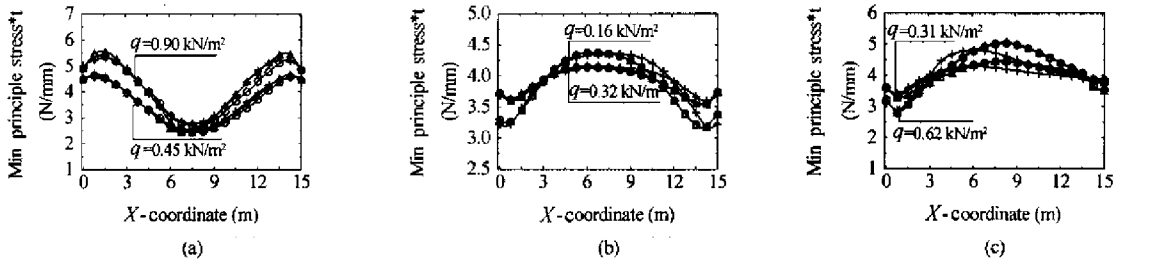

Fig.8 Minimum principle stress distributions along diagonal BD (near the cable) in the three load cases (a) LC1, (b) LC2 and (c) LC3

—+— Model 1: Sharing nodes; —△— Model 2: Cable sliding ($\mu = 0$); —○— Model 3: Cable sliding ($\mu = 0.7$)

Figs.7 – 8 demonstrated that: there was no distinct difference between the minimum/maximum principal stresses predicted by Model 2 and Model 3. The friction included in Model 3 had little influence on the stress distributions in the membrane. The stress distributions predicted by Model 1 deviated from those by Model 2 and Model 3, but the influences of the stress deviations on the load carrying capacity can be expected to be negligible (e.g. Load Case 1 in Table 1), as it modified the entire stress distributions only slightly.

Fig.9 shows the tensile forces in the cables predicted by the three analysis models for various load levels. The observed phenomena were similar to those for the stress distributions in the membrane. There were no distinct differences among the three analysis models for uniformly distributed upward and downward loads. For LC3, the differences between Model 1 and other two models seemed to be great when the loads approached the ultimate values. The phenomenon that part of the cable elements sagged while other cable elements are still tensioned can be clearly observed in LC3 for Model 1 (Fig.9c).

In Model 1, the cable elements shared the nodes with the membrane node. This assumption constrained the cable to re-distribute the forces uniformly along the cable length as in Model 2. When membrane structures are subjected to non-uniform loads, the forces in the cable along the length are non-uniform. As a result, one of the cable elements will sag prematurely and withdraw from the load carrying system, while the other cable elements still have high tensile forces. The load when one cable element sags is definitely smaller than that when all cable elements sag. From this point of view, it can be concluded that the loads predicted by Model 1 corresponding to cable sagging cannot be larger than those in

Model 2 and Model 3. Sometimes, the former could be much smaller than the latter, as demonstrated in Table 1 for LC3.

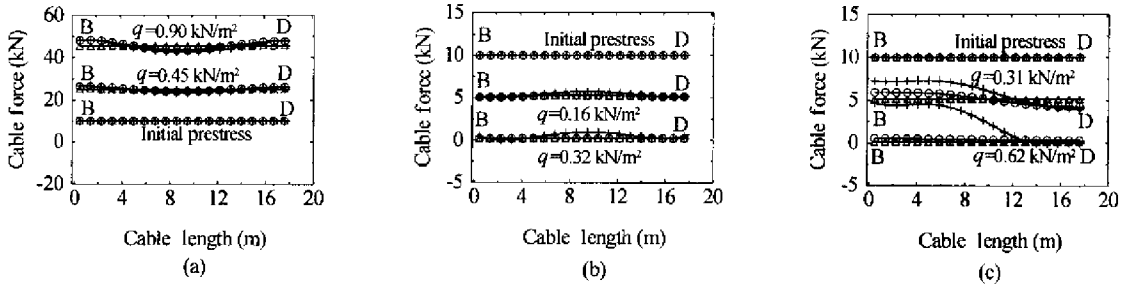

Fig.9 Influence of the three analysis models on cable forces (a) LC1, (b) LC2 and (c) LC3

—+— Model 1: Sharing nodes; —△— Model 2: Cable sliding ($\mu = 0$); —○— Model 3: Cable sliding ($\mu = 0.7$)

In Model 3, the cable forces along the length were also non-uniform due to the friction between the cable and the membrane. However, the friction only had small influence on the distribution of the cable forces (Fig. 9). As a result, this kind of non-uniformity did not influence the stress distributions in the membrane remarkably (Figs. 7 – 8). The load carrying capacity determined by Model 3 was almost the same as that by Model 2 (Table 1).

3. Influences of cable sliding on structure deformations

Fig. 10 compares the influences of the three analysis models on the deformations in the membrane. The figure demonstrates that there is no distinct difference between the results predicted by the three analysis models except for the zone near the cable. Fig. 11 shows the cable displacements. Only a little difference was observed when

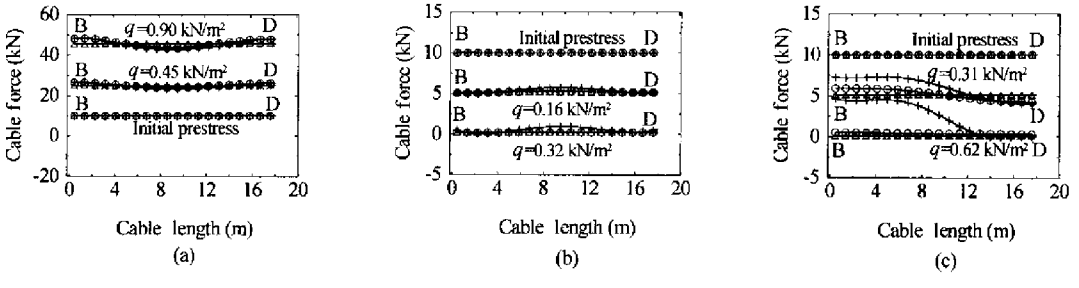

Fig.10 Influence of analysis models on the membrane deformations (a) LC1, (b) LC2 and (c) LC3 along diagonal AC

—+— Model 1: Sharing nodes; —△— Model 2: Cable sliding ($\mu = 0$); —○— Model 3: Cable sliding ($\mu = 0.7$)

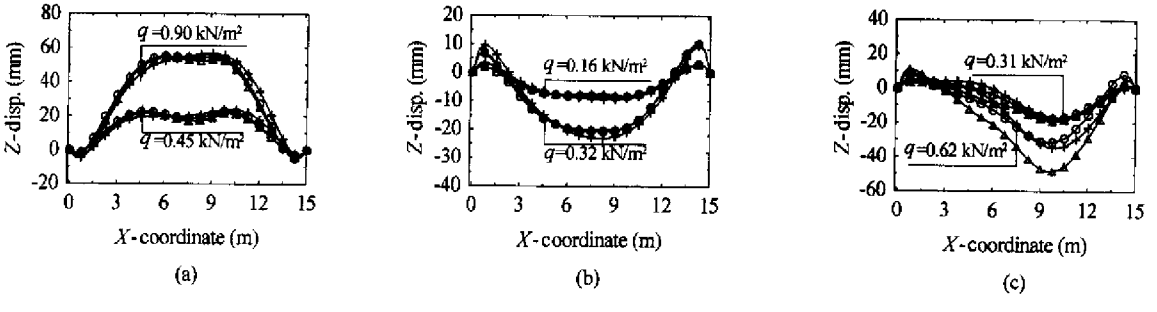

Fig.11 Influence of analysis models on the cable deformations (a) LC1, (b) LC2 and (c) LC3

—+— Model 1: Sharing nodes; —△— Model 2: Cable sliding ($\mu = 0$); —○— Model 3: Cable sliding ($\mu = 0.7$)

the structures were subjected to uniformly distributed loads (Figs. 11a – 11b). The existence of friction between the membrane and the cable reduced the cable displacements, especially when the structures were subjected to non-uniformly distributed loads (Fig. 11c). The same was found for the relative sliding between the membrane and the cable (Table 2). Table 2 compares the maximum accumulated relative sliding of the cable on the membrane surface along (CSLIP1) and transverse to (CSLIP2) the cable.

Table 2 Comparison of relative cable sliding on the membrane surface (mm)

	CSLIP1		CSLIP2	
	$\mu=0.0$	$\mu=0.7$	$\mu=0.0$	$\mu=0.7$
LC1	6.0	0.80	15	0.85
LC2	4.4	1.1	5.8	0.70
LC3	51.8	7.4	90.0	5.5

Fig. 12 shows the deformation pattern predicted by Model 3 for LC3 when the load closed to the ultimate load. The deformation magnification factor is 5.

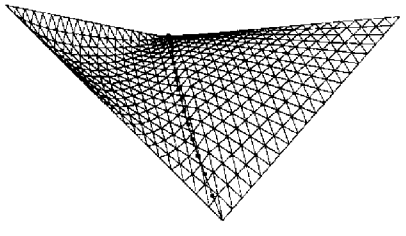

Fig. 12 Deformation of the tensioned membrane structure under LC3 at the incipient cable sagging

NATURAL VIBRATION ANALYSIS

Similar to the load deflection analysis, the same three analysis models were employed. Table 3 compares the influence of the analysis models on the lowest four natural frequencies.

Table 3 Influence of analysis models on the natural frequency (Hz)

	Mode 1	Mode 2	Mode 3	Mode 4
Model 1	7.19	7.72	8.39	8.57
Model 2	3.30	6.22	7.17	7.74
Model 3	7.19	7.74	8.40	8.61

Table 3 shows Model 1 and Model 3 presenting almost identical frequencies, while there is a great difference between Model 2 and the other two models. Observing the corresponding modes (Figs. 13 – 15), it could be found that the first two modes for Model 2 are the vibrations of the cables on the membrane surface. Though the membrane contributes to the vibration of the second mode, the cable vibration dominated the modes. For higher modes, the situation is reversed and the cable sliding seemed to have little influence on the frequencies and the modes. It is interesting to note that the third to fourth modes predicted by Model 2 had almost identical frequencies and modes to the lowest four frequencies and modes predicted by Models 1 and 3.

In Model 1, the assumption was that the membrane elements shared the nodes with the cable elements constraining the cable to vibrate freely on the membrane surface; so the vibration

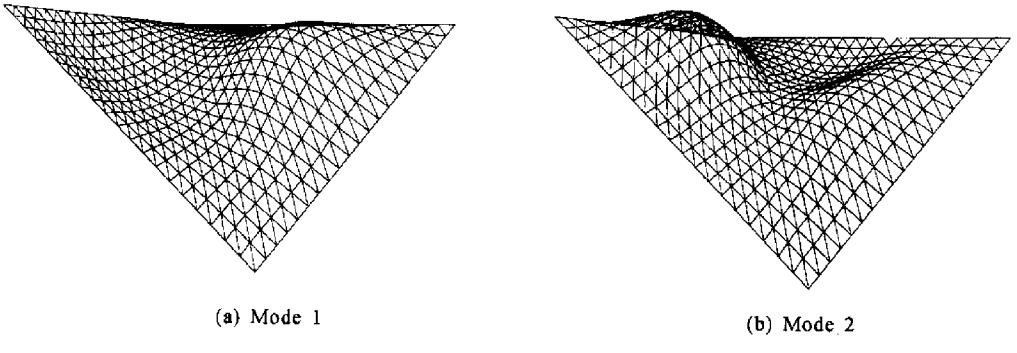

(a) Mode 1 (b) Mode 2

Fig. 13 The vibration modes (a & b) of the membrane structure based on Model 1: Sharing nodes

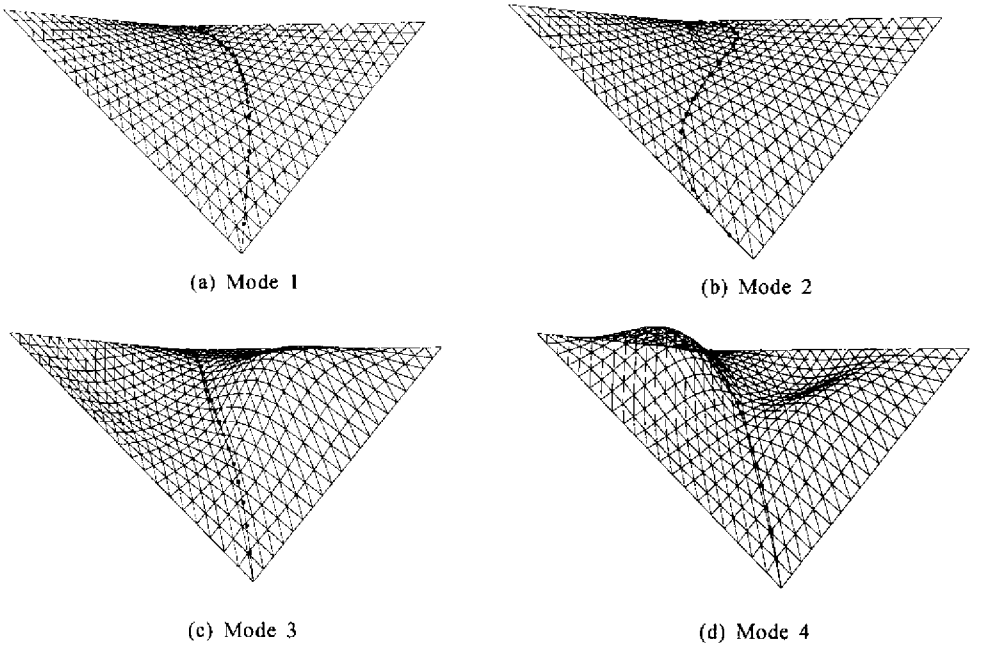

Fig.14 The vibration modes(a, b, c and d) of the membrane structure based on Model 2: Cable sliding ($\mu = 0$)

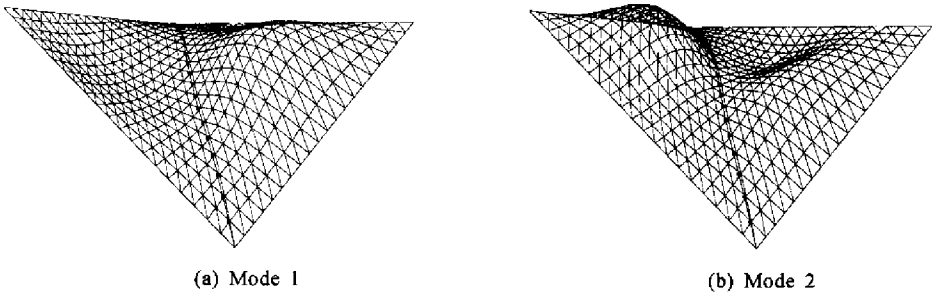

Fig.15 The vibration modes(a & b) of the membrane structure based on Model 3: Cable sliding ($\mu = 0.7$)

of the membrane dominated the vibration modes. For Model 3, the friction between the cable and the membrane had similar constraint on the cable. This led to the agreement of the frequencies predicted with two different analysis models. In Fig.15, the phenomenon that the cable elements did not coincide with the membrane side did not mean that there was sliding during the vibration. It follows from the shape-finding analysis. Careful check of the output files also demonstrated that there was no sliding between the cable and the membrane during the calculation of eigenvalues by Model 3.

On the other hand, if a small friction value was included in analysis Model 2, e.g. the coefficient of the friction $\mu = 0.01$, the frequencies and the corresponding vibration modes were the same as those by Model 1 and Model 3. Thus whether friction is included or not was of utmost important for the calculation of eigenvalues for natural frequencies, although the frequencies were found to be insensitive to the value of the non-zero coefficient of the friction.

REMARKS AND LIMITATIONS

In the present paper, the general finite element code ABAQUS was employed to investigate the influence of cable sliding on membrane surface on the structure shape, static and dynamic

behavior. Three analysis models were devised to fulfill this purpose. The investigation yielded satisfactory results. Cable sliding only affects deformations of the membrane near the cable arrangements. It did not change the overall view of the structure configuration. The influences on the stress states of the membrane were much smaller than on the deformations, so they could be ignored. The friction between the cable and the membrane surface could reduce cable sliding on the membrane surface, but had no influence on structure shapes and static behavior. The loads corresponding to membrane wrinkling were the same for the three analysis models. If cable sagging was regarded as the criteria of failure, Model 1 (the membrane element sharing nodes with the cable element) presented conservative load carrying capacity.

The influence of the cable sliding on the dynamic behavior was twofold. When the cable could slide without friction on the membrane surface, it could vibrate freely on the membrane surface. The vibration modes and the frequencies were different from those predicted with other analysis models. When the friction between the cable and the membrane was taken into consideration, no matter how small the friction was, there was no difference whether the cable could slide on the membrane surface or share the nodes with the membrane. For practical membrane structures, friction is inevitable though the coefficient between the coated membrane and the cable may be small. Thus cable sliding can be ignored again.

Cable sliding has little influence on the performance of tensioned membrane structures. A more simple analysis model (assuming the membrane elements share nodes with the cable elements) can be employed to analyze the membrane structures for simplicity, with the accuracy being guaranteed.

The type of cables discussed in the present study can be observed frequently in tensioned membrane structures. One of the main purposes of such cables is to strengthen or to stabilize the membrane structures under the action of wind loads. In this situation, wind-induced response analysis is required. The present analyses can be regarded as starting points for further investigation.

The above conclusions were based on the analysis results of a typical saddle-shaped membrane structure. The analyses did not take material failure into considerations; this simplification is based on observations that the maximum principal stresses during the load-deflection analyses (Fig.7) were almost the same for the three analysis models. Thus, if material failure occurs prior to the membrane wrinkling and cable sagging, the three analytical models are supposed to give identical load carrying capacity.

References

Argyris, J., Angelopoulos, J. and Bichat, B., 1974. A general method for the shape finding of lightweight tension structures. *Comput. Methods Appl. Mech. Engrg.*, **3**: 135 – 149.

Bletzinger, K.U. and Ramm, E., 1999. A general finite element approach to the form finding of tensile structures by the updated reference strategy. *Int. J. Space Structures*, **14**(2): 131 – 145.

Day, A.S. and Bunce, J., 1969. The analysis of hanging roofs. *Arup Journal*, 1969(Sept): 30 – 31.

Haug, E. and Powell, G.H., 1971. Finite Element Analysis of Nonlinear Membrane Structures. Proc., IASS Symposium Pacific Part II on Tension Structures and Space Frames, Tokyo and Kyoto, p.165 – 175.

HKS, 2000. ABAQUS User's Manual, Ver. 6.1. Hibbitt, Karlsson and Sorensen Inc., USA.

Ishii, K., 1999. Form finding analysis in consideration of cutting patterns of membrane structures. *Int. J. Space Structures*, **14**(2): 105 – 120.

Lewis, W.J. and Lewis, T.S., 1996. Application of Formian and dynamic relaxation to the form finding of minimal surfaces. *J. of the IASS*, **37**(3): 165 – 186.

Matsumura, T., Oda, K. and Tachibana, E., 1997. Finite Element Analysis of Cable Reinforced Membrane Structures With the Use of Bendable-Element. Proc., IASS Int. Symposium '97 on Shell & Spatial Structures, Singapore, **2**: 567 – 576.

Meek, J.L. and Xia, X.Y., 1999. Computer shape finding of form structures. *Int. J. Space Structures*, **14**(1): 35 – 55.

Minami, H., Yamamoto, C., Segawa, S. and Kono, Y., 1997. A Method for Membrane Material Nonlinear Stress Analysis Using A Multi-Step Linear approximation. Proc., IASS Int. Symposium '97 on Shell & Spatial Structures, Singapore, **2**: 595 – 602.

Otto, F., 1973. Tensile Structures. Vols. 1 and 2, MIT, Cambridge, MA.

Schek, H.J., 1974. The force density method for form finding and computations of general networks. *Comp. Methods Appl. Mech. Engrg.*, **3**: 115 – 134.